

A Toroidal Maxwell–Cremona–Delaunay Correspondence*

Jeff Erickson Patrick Lin

University of Illinois, Urbana-Champaign

Submitted to *Journal of Computational Geometry* — July 31, 2020

Abstract

We consider three classes of geodesic embeddings of graphs on Euclidean flat tori:

- A torus graph G is *equilibrium* if it is possible to place positive weights on the edges, such that the weighted edge vectors incident to each vertex of G sum to zero.
- A torus graph G is *reciprocal* if there is a geodesic embedding of the dual graph G^* on the same flat torus, where each edge of G is orthogonal to the corresponding dual edge in G^* .
- A torus graph G is *coherent* if it is possible to assign weights to the vertices, so that G is the (intrinsic) weighted Delaunay graph of its vertices.

The classical Maxwell–Cremona correspondence and the well-known correspondence between convex hulls and weighted Delaunay triangulations imply that the analogous concepts for plane graphs (with convex outer faces) are equivalent. Indeed, all three conditions are equivalent to G being the projection of the 1-skeleton of the lower convex hull of points in \mathbb{R}^3 . However, this three-way equivalence does not extend directly to geodesic graphs on flat tori. On any flat torus, reciprocal and coherent graphs are equivalent, and every reciprocal graph is equilibrium, but not every equilibrium graph is reciprocal. We establish a weaker correspondence: Every equilibrium graph on any flat torus is affinely equivalent to a reciprocal/coherent graph on *some* flat torus.

*Portions of this work were supported by NSF grant CCF-1408763. A preliminary version of this paper was presented at the 36th International Symposium on Computational Geometry [33].

1 Introduction

The Maxwell–Cremona correspondence is a fundamental theorem establishing an equivalence between three different structures on straight-line graphs G in the plane:

- An *equilibrium stress* on G is an assignment of non-zero weights to the edges of G , such that the weighted edge vectors around every interior vertex p sum to zero:

$$\sum_{p: pq \in E} \omega_{pq}(p - q) = \begin{pmatrix} 0 \\ 0 \end{pmatrix}$$

- A *reciprocal diagram* for G is a straight-line drawing of the dual graph G^* , in which every edge e^* is orthogonal to the corresponding primal edge e .
- A *polyhedral lifting* of G assigns z -coordinates to the vertices of G , so that the resulting lifted vertices in \mathbb{R}^3 are not all coplanar, but the lifted vertices of each face of G are coplanar.

Building on earlier seminal work of Varignon [83], Rankine [68, 69], and others, Maxwell [55–57] proved that any straight-line planar graph G with an equilibrium stress has both a reciprocal diagram and a polyhedral lifting. In particular, positive and negative stresses correspond to convex and concave edges in the polyhedral lifting, respectively. Moreover, for any equilibrium stress ω on G , the vector $1/\omega$ is an equilibrium stress for the reciprocal diagram G^* . Finally, for any polyhedral liftings of G , one can obtain a polyhedral lifting of the reciprocal diagram G^* via projective duality. Maxwell’s analysis was later extended and popularized by Cremona [25, 26] and others; the correspondence has since been rediscovered several times in other contexts [3, 41]. More recently, Whiteley [85] proved the converse of Maxwell’s theorem: every reciprocal diagram and every polyhedral lift corresponds to an equilibrium stress; see also Crapo and Whiteley [24]. For modern expositions of the Maxwell–Cremona correspondence aimed at computational geometers, see Hopcroft and Kahn [40], Richter-Gebert [71, Chapter 13], or Rote, Santos, and Streinu [73].

If the outer face of G is convex, the Maxwell–Cremona correspondence implies an equivalence between equilibrium stresses in G that are *positive* on every interior edge, *convex* polyhedral liftings of G , and reciprocal *embeddings* of G^* . Moreover, as Whiteley *et al.* [86] and Aurenhammer [3] observed, the well-known equivalence between convex liftings and weighted Delaunay complexes [4, 5, 13, 32, 84] implies that all three of these structures are equivalent to a fourth:

- A *Delaunay weighting* of G is an assignment of weights to the vertices of G , so that G is the (power-)weighted Delaunay graph [4, 7] of its vertices.

Among many other consequences, combining the Maxwell–Cremona correspondence [85] with Tutte’s spring-embedding theorem [82] yields an elegant geometric proof of Steinitz’s theorem [76, 77] that every 3-connected planar graph is the 1-skeleton of a 3-dimensional convex polytope. The Maxwell–Cremona correspondence has been used for scene analysis of planar drawings [3, 5, 24, 41, 81], finding small grid embeddings of planar graphs and polyhedra [15, 30, 31, 42, 66, 70, 71, 74], and several linkage reconfiguration problems [22, 29, 67, 79, 80].

It is natural to ask how or whether these correspondences extend to graphs on surfaces other than the Euclidean plane. Lovász [52, Lemma 4] describes a spherical analogue of Maxwell’s polyhedral lifting in terms of Colin de Verdière matrices [17, 20]; see also [47]. Izvestiev [45] provides a self-contained proof of the correspondence for planar frameworks, along with natural extensions to frameworks in the sphere and the hyperbolic plane. Finally, and most closely related to the present work, Borcea

and Streinu [11], building on their earlier study of rigidity in infinite periodic frameworks [9, 10], develop an extension of the Maxwell–Cremona correspondence to infinite periodic graphs in the plane, or equivalently, to geodesic graphs on the Euclidean flat torus. Specifically, Borcea and Streinu prove that *periodic* polyhedral liftings correspond to *periodic* stresses satisfying an additional homological constraint.¹

1.1 Our Results

In this paper, we develop a different generalization of the Maxwell–Cremona–Delaunay correspondence to geodesic embeddings of graphs on Euclidean flat tori. Our work is inspired by and uses Borcea and Streinu’s results [11], but considers a different aim. Stated in terms of infinite periodic planar graphs, Borcea and Streinu study periodic equilibrium stresses, which necessarily include both positive and negative stress coefficients, that include periodic *polyhedral lifts*; whereas, we are interested in periodic *positive* equilibrium stresses that induce periodic reciprocal *embeddings* and periodic *Delaunay weights*. This distinction is aptly illustrated in Figures 8–10 of Borcea and Streinu’s paper [11].

Recall that a Euclidean flat torus \mathbb{T} is the metric space obtained by identifying opposite sides of an arbitrary parallelogram in the Euclidean plane. A *geodesic* graph G in the flat torus \mathbb{T} is an embedded graph where each edge is represented by a “line segment”. Equilibrium stresses, reciprocal embeddings, and weighted Delaunay graphs are all well-defined in the intrinsic metric of the flat torus. We prove the following correspondences for any geodesic graph G on any flat torus \mathbb{T} .

- Any equilibrium stress for G is also an equilibrium stress for the affine image of G on any other flat torus \mathbb{T}' (Lemma 2.2). Equilibrium depends only on the common *affine* structure of all flat tori.
- Any reciprocal embedding G^* on \mathbb{T} —that is, any geodesic embedding of the dual graph such that corresponding edges are orthogonal—defines unique equilibrium stresses in both G and G^* (Lemma 3.1).
- G has a reciprocal embedding if and only if G is coherent. Specifically, each reciprocal diagram for G induces an essentially unique set of Delaunay weights for the vertices of G (Theorem 4.5). Conversely, each set of Delaunay weights for G induces a *unique* reciprocal diagram G^* , namely the corresponding weighted Voronoi diagram (Lemma 4.1). Thus, unlike in the plane, a reciprocal diagram G^* may not be a weighted Voronoi diagram of the vertices of G , but some unique translation of G^* is.
- Unlike in the plane, G may have equilibrium stresses that are not induced by reciprocal embeddings; more generally, not every equilibrium graph on \mathbb{T} is reciprocal (Theorem 3.2). Unlike equilibrium, reciprocity depends on the *conformal* structure of \mathbb{T} , which is determined by the shape of its fundamental parallelogram. We derive a simple geometric condition that characterizes which equilibrium stresses are reciprocal on \mathbb{T} (Lemma 5.5).
- More generally, we show that for any equilibrium stress on G , there is a flat torus \mathbb{T}' , unique up to rotation and scaling of its fundamental parallelogram, such that the same equilibrium stress is reciprocal for the affine image of G on \mathbb{T}' (Theorem 5.8). In short, every equilibrium stress for G is reciprocal on *some* flat torus. This result implies a natural toroidal analogue of Steinitz’s theorem

¹Phrased in terms of toroidal frameworks, Borcea and Streinu consider only equilibrium stresses for which the corresponding reciprocal toroidal framework contains no essential cycles. The same condition was also briefly discussed by Crapo and Whiteley [24, Example 3.6].

(Theorem 6.1): Every essentially 3-connected torus graph G is homotopic to a weighted Delaunay graph on some flat torus.

1.2 Other Related Results

Our results rely on a natural generalization (Theorem 2.3) of Tutte’s spring-embedding theorem to the torus, first proved (in much greater generality) by Colin de Verdière [18], and later proved again, in different forms, by Delgado-Friedrichs [28], Lovász [53, Theorem 7.1] [54, Theorem 7.4], and Gortler, Gotsman, and Thurston [36]. Steiner and Fischer [75] and Gortler *et al.* [36] observed that this toroidal spring embedding can be computed by solving the Laplacian linear system defining the equilibrium conditions. We describe this result and the necessary calculation in more detail in Section 2. Equilibrium and reciprocal graph embeddings can also be viewed as discrete analogues of harmonic and holomorphic functions [53, 54].

Our weighted Delaunay graphs are (the duals of) *power diagrams* [4, 6] or *Laguerre-Voronoi diagrams* [43] in the intrinsic metric of the flat torus. Toroidal Delaunay triangulations are commonly used to generate finite-element meshes for simulations with periodic boundary conditions, and several efficient algorithms for constructing these triangulations are known [8, 14, 37, 59]. Building on earlier work of Rivin [72] and Indermitte *et al.* [44], Bobenko and Springborn [7] proved that on any piecewise-linear surface, intrinsic Delaunay triangulations can be constructed by an intrinsic incremental flipping algorithm, mirroring the classical planar algorithm of Lawson [51]; their analysis extends easily to intrinsic weighted Delaunay graphs. Weighted Delaunay complexes are also known as *regular* or *coherent* subdivisions [27, 87].

Finally, equilibrium and reciprocal embeddings are closely related to the celebrated Koebe-Andreev circle-packing theorem: Every planar graph is the contact graph of a set of interior-disjoint circular disks [1, 2, 46]; see Felsner and Rote [34] for a simple proof, based in part on earlier work of Brightwell and Scheinerman [12] and Mohar [60]. The circle-packing theorem has been generalized to higher-genus surfaces by Colin de Verdière [16, 19] and Mohar [61, 62]. In particular, Mohar proves that any well-connected graph G on the torus is *homotopic* to an essentially unique circle packing for a unique Euclidean metric on the torus. This disk-packing representation immediately yields a weighted Delaunay graph, where the areas of the disks are the vertex weights. We revisit and extend this result in Section 6.

Discrete harmonic and holomorphic functions, circle packings, and intrinsic Delaunay triangulations have numerous applications in discrete differential geometry; we refer the reader to monographs by Crane [23], Lovász [54], and Stephenson [78].

2 Background and Definitions

2.1 Flat Tori

A *flat torus* is the metric surface obtained by identifying opposite sides of a parallelogram in the Euclidean plane. Specifically, for any nonsingular 2×2 matrix $M = \begin{pmatrix} a & b \\ c & d \end{pmatrix}$, let \mathbb{T}_M denote the flat torus obtained by identifying opposite edges of the *fundamental parallelogram* \diamond_M with vertex coordinates $\begin{pmatrix} 0 \\ 0 \end{pmatrix}$, $\begin{pmatrix} a \\ c \end{pmatrix}$, $\begin{pmatrix} b \\ d \end{pmatrix}$, and $\begin{pmatrix} a+b \\ c+d \end{pmatrix}$. In particular, the *square* flat torus $\mathbb{T}_\square = \mathbb{T}_I$ is obtained by identifying opposite sides of the Euclidean unit square $\square = \diamond_I = [0, 1]^2$. The linear map $M: \mathbb{R}^2 \rightarrow \mathbb{R}^2$ naturally induces a homeomorphism from \mathbb{T}_\square to \mathbb{T}_M .

Equivalently, \mathbb{T}_M is the quotient space of the plane \mathbb{R}^2 with respect to the lattice Γ_M of translations generated by the columns of M ; in particular, the square flat torus is the quotient space $\mathbb{R}^2/\mathbb{Z}^2$. The quotient map $\pi_M: \mathbb{R}^2 \rightarrow \mathbb{T}_M$ is called a *covering map* or *projection*. A *lift* of a point $p \in \mathbb{T}_M$ is any

point in the preimage $\pi_M^{-1}(p) \subset \mathbb{R}^2$. A **geodesic** in \mathbb{T}_M is the projection of any line segment in \mathbb{R}^2 ; we emphasize that geodesics are *not* necessarily shortest paths.

2.2 Graphs and Embeddings

We regard each edge of an undirected graph G as a pair of opposing **darts**, each directed from one endpoint, called the **tail** of the dart, to the other endpoint, called its **head**. For each edge e , we arbitrarily label the darts e^+ and e^- ; we call e^+ the **reference dart** of e . We explicitly allow graphs with loops and parallel edges. At the risk of confusing the reader, we often write $p \rightarrow q$ to denote an arbitrary dart with tail p and head q , and $q \rightarrow p$ for the reversal of $p \rightarrow q$.

A **drawing** of a graph G on a torus \mathbb{T} is any continuous function from G (as a topological space) to \mathbb{T} . An **embedding** is an injective drawing, which maps vertices of G to distinct points and edges to interior-disjoint simple paths between their endpoints. The **faces** of an embedding are the components of the complement of the image of the graph; we consider only **cellular** embeddings, in which all faces are open disks. (Cellular graph embeddings are also called *maps*.) We typically do not distinguish between vertices and edges of G and their images in any embedding; we will informally refer to any embedded graph on any flat torus as a **torus graph**.

In any embedded graph, **left(d)** and **right(d)** denote the faces immediately to the left and right of any dart d . (These are possibly the same face.)

The **universal cover** \tilde{G} of an embedded graph G on any flat torus \mathbb{T}_M is the unique infinite periodic graph in \mathbb{R}^2 such that $\pi_M(\tilde{G}) = G$; in particular, each vertex, edge, or face of \tilde{G} projects to a vertex, edge, or face of G , respectively. A torus graph G is **essentially simple** if its universal cover \tilde{G} is simple, and **essentially 3-connected** if \tilde{G} is 3-connected [35, 61–64]. We emphasize that essential simplicity and essential 3-connectedness are features of *embeddings*, not of abstract graphs; see Figure 1.

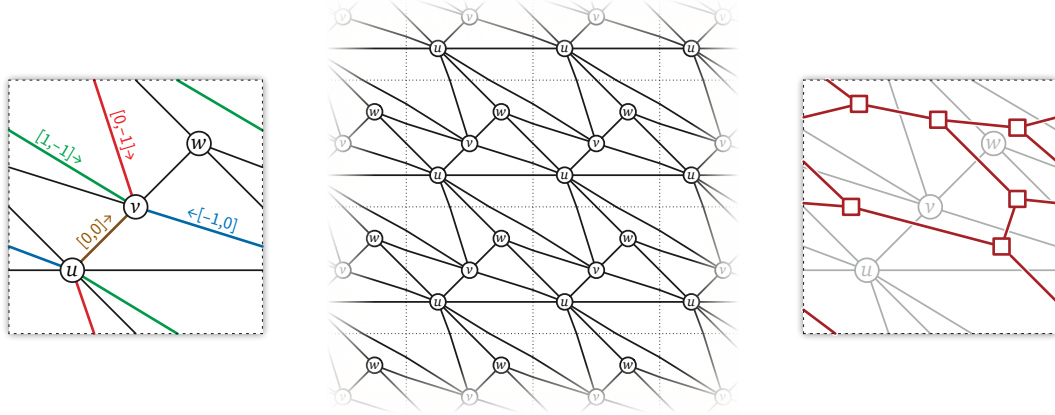


Figure 1. An essentially simple, essentially 3-connected geodesic graph on the square flat torus (showing the homology vectors of all four darts from u to v), a small portion of its universal cover, and its dual graph

2.3 Homology, Homotopy, and Circulations

For any embedding of a graph G on the square flat torus \mathbb{T}_{\square} , we associate a **homology vector** $[d] \in \mathbb{Z}^2$ with each dart d , which records how the dart crosses the boundary edges of the unit square. Specifically, the first coordinate of $[d]$ is the number of times d crosses the vertical boundary rightward, minus the number of times d crosses the vertical boundary leftward; and the second coordinate of $[d]$ is the number of times d crosses the horizontal boundary upward, minus the number of times d crosses the horizontal boundary downward. In particular, reversing a dart negates its homology vector: $[e^+] = -[e^-]$. Again,

see Figure 1. For graphs on any other flat torus \mathbb{T}_M , homology vectors of darts are similarly defined by how they crosses the edges of the fundamental parallelogram \diamond_M .

The **(integer) homology class** $[\gamma]$ of a directed cycle γ in G is the sum of the homology vectors of its forward darts. A cycle is *contractible* if its homology class is $\begin{pmatrix} 0 \\ 0 \end{pmatrix}$ and *essential* otherwise. In particular, the boundary cycle of each face of G is contractible.

Two cycles on a torus \mathbb{T} are **homotopic** if one can be continuously deformed into the other, or equivalently, if they have the same integer homology class. Similarly, two drawings of the same graph G on the same flat torus \mathbb{T} are homotopic if one can be continuously deformed into the other. Two drawings of the same graph G on the same flat torus \mathbb{T} are homotopic if and only if every cycle has the same homology class in both embeddings [21, 50].

A **circulation** ϕ in G is a function from the darts of G to the reals, such that $\phi(p \rightarrow q) = -\phi(q \rightarrow p)$ for every dart $p \rightarrow q$ and $\sum_{p \rightarrow q} \phi(p \rightarrow q) = 0$ for every vertex p . We represent circulations by column vectors in \mathbb{R}^E , indexed by the edges of G , where $\phi_e = \phi(e^+)$. Let Λ denote the $2 \times E$ matrix whose columns are the homology vectors of the reference darts in G . The homology class of a circulation is the matrix-vector product

$$[\phi] = \Lambda \phi = \sum_{e \in E} \phi(e^+) \cdot [e^+].$$

(This identity directly generalizes our earlier definition of the homology class $[\gamma]$ of a cycle γ .)

2.4 Geodesic Drawings and Embeddings

A **geodesic drawing** of G on any flat torus \mathbb{T}_M is a drawing that maps edges to geodesics; similarly, a **geodesic embedding** is an embedding that maps edges to geodesics. Equivalently, an embedding is geodesic if its universal cover \tilde{G} is a straight-line plane graph.

A geodesic drawing of G in \mathbb{T}_M is uniquely determined by its **coordinate representation**, which consists of a coordinate vector $\langle p \rangle \in \diamond_M$ for each vertex p , together with the homology vector $[e^+] \in \mathbb{Z}^2$ of each edge e .

The **displacement vector** Δ_d of any dart d is the difference between the head and tail coordinates of any lift of d in the universal cover \tilde{G} . Displacement vectors can be equivalently defined in terms of vertex coordinates, homology vectors, and the shape matrix M as follows:

$$\Delta_{p \rightarrow q} := \langle q \rangle - \langle p \rangle + M[p \rightarrow q].$$

Reversing a dart negates its displacement: $\Delta_{q \rightarrow p} = -\Delta_{p \rightarrow q}$. We sometimes write Δx_d and Δy_d to denote the first and second coordinates of Δ_d . The **displacement matrix** Δ of a geodesic drawing is the $2 \times E$ matrix whose columns are the displacement vectors of the reference darts of G . Every geodesic drawing on \mathbb{T}_M is determined *up to translation* by its displacement matrix.

On the *square* flat torus, the integer homology class of any directed cycle is also equal to the sum of the *displacement* vectors of its darts:

$$[\gamma] = \sum_{p \rightarrow q \in \gamma} [p \rightarrow q] = \sum_{p \rightarrow q \in \gamma} \Delta_{p \rightarrow q}.$$

In particular, the total displacement of any contractible cycle is zero, as expected. Extending this identity to circulations by linearity gives us the following useful lemma:

Lemma 2.1. *Fix a geodesic drawing of a graph G on \mathbb{T}_{\square} with displacement matrix Δ . For any circulation ϕ in G , we have $\Delta \phi = \Lambda \phi = [\phi]$.*

2.5 Equilibrium Stresses and Spring Embeddings

A **stress** in a geodesic torus graph G is a real vector $\omega \in \mathbb{R}^E$ indexed by the edges of G . Unlike circulations, homology vectors, and displacement vectors, stresses can be viewed as *symmetric* functions on the *darts* of G . An **equilibrium stress** in G is a stress ω that satisfies the following identity at every vertex p :

$$\sum_{p \rightarrow q} \omega_{pq} \Delta_{p \rightarrow q} = \begin{pmatrix} 0 \\ 0 \end{pmatrix}.$$

Unlike Borcea and Streinu [9–11], we consider only **positive** equilibrium stresses, where $\omega_e > 0$ for every edge e . It may be helpful to imagine each stress coefficient ω_e as a linear spring constant; intuitively, each edge pulls its endpoints inward, with a force equal to the length of e times the stress coefficient ω_e .

Recall that the linear map $M: \mathbb{R}^2 \times \mathbb{R}^2$ associated with any nonsingular 2×2 matrix induces a homeomorphism $\underline{M}: \mathbb{T}_\square \rightarrow \mathbb{T}_M$. In particular, applying this homeomorphism to a geodesic graph in \mathbb{T}_\square with displacement matrix Δ yields a geodesic graph on \mathbb{T}_M with displacement matrix $M\Delta$. Routine definition-chasing now implies the following lemma.

Lemma 2.2. *Let G be a geodesic graph on the square flat torus \mathbb{T}_\square . If ω is an equilibrium stress for G , then ω is also an equilibrium stress for the image of G on any other flat torus \mathbb{T}_M .*

Our results rely on the following natural generalization of Tutte’s spring embedding theorem to flat torus graphs.

Theorem 2.3 (Colin de Verdière [18]; see also [28, 36, 53]). *Let G be any essentially simple, essentially 3-connected embedded graph on any flat torus \mathbb{T} , and let ω be any positive stress on the edges of G . Then G is homotopic to a geodesic embedding in \mathbb{T} that is in equilibrium with respect to ω ; moreover, this equilibrium embedding is unique up to translation.*

Theorem 2.3 implies the following sufficient condition for a displacement matrix to describe a geodesic embedding on the square torus.

Lemma 2.4. *Fix an essentially simple, essentially 3-connected graph G on \mathbb{T}_\square , a $2 \times E$ matrix Δ , and a positive stress vector ω . Suppose for every directed cycle (and therefore any circulation) ϕ in G , we have $\Delta\phi = \Lambda\phi = [\phi]$. Then Δ is the displacement matrix of a geodesic **drawing** on \mathbb{T}_\square that is homotopic to G . If in addition ω is a positive equilibrium stress for that drawing, the drawing is an embedding.*

Proof: A classical result of Ladegaillerie [48–50] implies that two embeddings of the same graph on the same surface are isotopic if and only if every cycle has the same homology class in both embeddings. (See Colin de Verdière and de Mesmay [21].) Because homology and homotopy coincide on the torus, the assumption $\Delta\phi = \Lambda\phi = [\phi]$ for every directed cycle immediately implies that Δ is the displacement matrix of a geodesic drawing that is homotopic to G .

If ω is a positive equilibrium stress for that drawing, then the uniqueness clause in Theorem 2.3 implies that the drawing is in fact an embedding. \square

Following Steiner and Fischer [75] and Gortler, Gotsman, and Thurston [36], given the coordinate representation of any geodesic graph G on the square flat torus, with any positive stress vector $\omega > 0$, we can compute an isotopic equilibrium embedding of G by solving the linear system

$$\sum_{p \rightarrow q} \omega_{pq} (\langle q \rangle - \langle p \rangle + [p \rightarrow q]) = \begin{pmatrix} 0 \\ 0 \end{pmatrix} \quad \text{for every vertex } q \quad (2.1)$$

for the vertex locations $\langle p \rangle$, treating the homology vectors $[p \rightarrow q]$ as constants. Alternatively, Lemma 2.4 implies that we can compute the displacement vectors of every isotopic equilibrium embedding directly, by solving the linear system

$$\begin{aligned} \sum_{p \rightarrow q} \omega_{pq} \Delta_{p \rightarrow q} &= \begin{pmatrix} 0 \\ 0 \end{pmatrix} && \text{for every vertex } q \\ \sum_{\text{left}(d)=f} \Delta_d &= \begin{pmatrix} 0 \\ 0 \end{pmatrix} && \text{for every face } f \\ \sum_{d \in \gamma_1} \Delta_d &= [\gamma_1] \\ \sum_{d \in \gamma_2} \Delta_d &= [\gamma_2] \end{aligned}$$

where γ_1 and γ_2 are any two directed cycles with independent non-zero homology classes.

2.6 Duality and Reciprocity

Every embedded torus graph G defines a **dual graph** G^* whose vertices correspond to the faces of G , where two vertices in G are connected by an edge for each edge separating the corresponding pair of faces in G . This dual graph G^* has a natural embedding in which each vertex f^* of G^* lies in the interior of the corresponding face f of G , each edge e^* of G^* crosses only the corresponding edge e of G , and each face p^* of G^* contains exactly one vertex p of G in its interior. We regard any embedding of G^* to be *dual* to G if and only if it is homotopic to this natural embedding. Each dart d in G has a corresponding dart d^* in G^* , defined by setting $\text{head}(d^*) = \text{left}(d)^*$ and $\text{tail}(d^*) = \text{right}(d)^*$; intuitively, the dual of a dart in G is obtained by rotating the dart counterclockwise.

It will prove convenient to treat vertex coordinates, displacement vectors, homology vectors, and circulations in any dual graph G^* as row vectors. For any vector $v \in \mathbb{R}^2$ we define $v^\perp := (Jv)^T$, where $J := \begin{pmatrix} 0 & -1 \\ 1 & 0 \end{pmatrix}$ is the matrix for a 90° counterclockwise rotation. Note that $J^T = J^{-1} = -J$. Similarly, for any $2 \times n$ matrix A , we define $A^\perp := (JA)^T = -A^T J$.

Two dual geodesic graphs G and G^* on the same flat torus \mathbb{T} are **reciprocal** if every edge e in G is orthogonal to its dual edge e^* in G^* .

A **cocirculation** in G a row vector $\theta \in \mathbb{R}^E$ whose transpose describes a circulation in G^* . The cohomology class $[\theta]^*$ of any cocirculation is the transpose of the homology class of the circulation θ^T in G^* . Recall that Λ is the $2 \times E$ matrix whose columns are homology vectors of edges in G . Let λ_1 and λ_2 denote the first and second rows of Λ .

Lemma 2.5. *The row vectors λ_1 and λ_2 describe cocirculations in G with cohomology classes $[\lambda_1]^* = (0, 1)$ and $[\lambda_2]^* = (-1, 0)$.*

Proof: Without loss of generality, assume that G is embedded on the flat square torus \mathbb{T}_\square , with no vertices on the boundary of the fundamental square \square . Let γ_1 and γ_2 denote directed cycles in \mathbb{T}_\square (not in G) induced by the boundary edges of \square , directed respectively rightward and upward.

Let d_0, d_1, \dots, d_{k-1} be the sequence of darts in G that cross γ_2 from left to right, indexed by the upward order of their intersection points. Each dart d that appears in this sequence appears exactly $\lambda_1(d)$ times, once for each crossing. For each index i , we have $\text{left}(d_i) = \text{right}(d_{i+1 \bmod k})$; thus, the corresponding sequence of dual darts $d_0^*, d_1^*, \dots, d_{k-1}^*$ describes a closed walk in G^* . This closed walk can be continuously deformed to γ_2 , so it has the same homology class as γ_2 ; see Figure 2. We conclude that $[\lambda_1]^* = (0, 1)$.

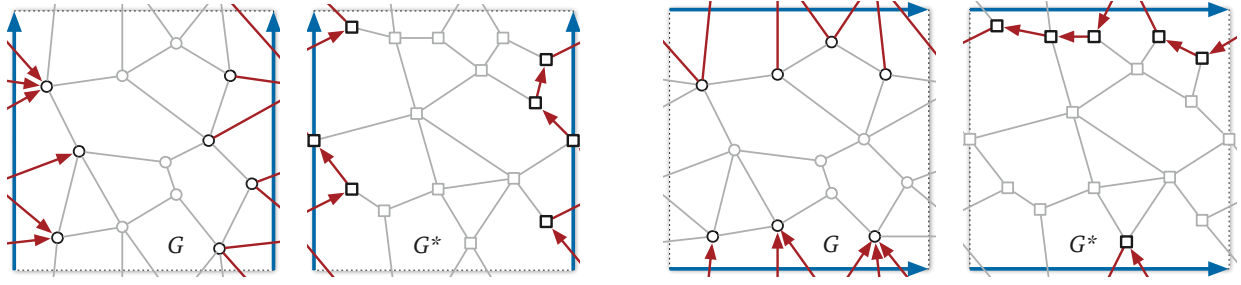


Figure 2. Proof of Lemma 2.5: The darts in G crossing either boundary edge of the fundamental square dualize to a closed walk in G^* parallel to that boundary edge.

Symmetrically, the darts crossing γ_1 upward define a closed walk in G^* in the same homology class as the reversal of γ_1 , and therefore $[\lambda_2]^* = (-1, 0)$. \square

2.7 Coherent Subdivisions

Let G be a geodesic graph in \mathbb{T}_M , and fix arbitrary real weights π_p for every vertex p of G . Let $p \rightarrow q$, $p \rightarrow r$, and $p \rightarrow s$ be three consecutive darts around a common tail p in clockwise order. Thus, $\text{left}(p \rightarrow q) = \text{right}(p \rightarrow r)$ and $\text{left}(p \rightarrow r) = \text{right}(p \rightarrow s)$. We call the edge pr **locally Delaunay** if the following determinant is positive:

$$\begin{vmatrix} \Delta x_{p \rightarrow q} & \Delta y_{p \rightarrow q} & \frac{1}{2}|\Delta_{p \rightarrow q}|^2 + \pi_p - \pi_q \\ \Delta x_{p \rightarrow r} & \Delta y_{p \rightarrow r} & \frac{1}{2}|\Delta_{p \rightarrow r}|^2 + \pi_p - \pi_r \\ \Delta x_{p \rightarrow s} & \Delta y_{p \rightarrow s} & \frac{1}{2}|\Delta_{p \rightarrow s}|^2 + \pi_p - \pi_s \end{vmatrix} > 0. \quad (2.2)$$

This inequality follows by elementary row operations and cofactor expansion from the standard determinant test for appropriate lifts of the vertices p, q, r, s to the universal cover:

$$\begin{vmatrix} 1 & x_p & y_p & \frac{1}{2}(x_p^2 + y_p^2) - \pi_p \\ 1 & x_q & y_q & \frac{1}{2}(x_q^2 + y_q^2) - \pi_q \\ 1 & x_r & y_r & \frac{1}{2}(x_r^2 + y_r^2) - \pi_r \\ 1 & x_s & y_s & \frac{1}{2}(x_s^2 + y_s^2) - \pi_s \end{vmatrix} > 0. \quad (2.3)$$

(The factor $1/2$ simplifies our later calculations, and is consistent with Maxwell’s construction of polyhedral liftings and reciprocal diagrams.) Similarly, we say that an edge is **locally flat** if the corresponding determinant is zero. Finally, G is the **weighted Delaunay graph** of its vertices if every edge of G is locally Delaunay and every diagonal of every non-triangular face is locally flat.

One can easily verify that this condition is equivalent to G being the projection of the weighted Delaunay graph of the lift $\pi_M^{-1}(V)$ of its vertices V to the universal cover. Results of Bobenko and Springborn [7] imply that any finite set of weighted points on any flat torus has a unique weighted Delaunay graph. We emphasize that weighted Delaunay graphs are *not* necessarily either simple or triangulations; however, every weighted Delaunay graphs on any flat torus is both essentially simple and essentially 3-connected. The dual **weighted Voronoi graph** of P , also known as its *power diagram* [4, 6], can be defined similarly by projection from the universal cover.

Finally, a geodesic torus graph is **coherent** if it is the weighted Delaunay graph of its vertices, with respect to some vector of weights.

3 Reciprocal Implies Equilibrium

Lemma 3.1. *Let G and G^* be reciprocal geodesic graphs on some flat torus \mathbb{T}_M . The vector ω defined by $\omega_e = |e^*|/|e|$ is an equilibrium stress for G ; symmetrically, the vector ω^* defined by $\omega_{e^*}^* = 1/\omega_e = |e|/|e^*|$ is an equilibrium stress for G^* .*

Proof: Let $\omega_e = |e^*|/|e|$ and $\omega_{e^*}^* = 1/\omega_e = |e|/|e^*|$ for each edge e . Let Δ denote the displacement matrix of G , and let Δ^* denote the (transposed) displacement matrix of G^* . We immediately have $\Delta_{e^*}^* = \omega_e \Delta_e^\perp$ for every edge e of G . The darts leaving each vertex p of G dualize to a facial cycle around the corresponding face p^* of G^* , and thus

$$\left(\sum_{q: pq \in E} \omega_{pq} \Delta_{p \rightarrow q} \right)^\perp = \sum_{q: pq \in E} \omega_{pq} \Delta_{p \rightarrow q}^\perp = \sum_{q: pq \in E} \Delta_{(p \rightarrow q)^*}^* = (0, 0).$$

We conclude that ω is an equilibrium stress for G , and thus (by swapping the roles of G and G^*) that ω^* is an equilibrium stress for G^* . \square

A stress vector ω is a **reciprocal stress** for G if there is a reciprocal graph G^* on the same flat torus such that $\omega_e = |e^*|/|e|$ for each edge e . Thus, a geodesic torus graph is reciprocal if and only if it has a reciprocal stress, and Lemma 3.1 implies that every reciprocal stress is an equilibrium stress. The following simple construction shows that the converse of Lemma 3.1 is false.

Theorem 3.2. *Not every positive equilibrium stress for G is a reciprocal stress. More generally, not every equilibrium graph on \mathbb{T} is reciprocal/coherent on \mathbb{T} .*

Proof: Let G_1 be the geodesic triangulation in the flat square torus \mathbb{T}_\square with a single vertex p and three edges, whose reference darts have displacement vectors $\begin{pmatrix} 1 \\ 0 \end{pmatrix}$, $\begin{pmatrix} 1 \\ 1 \end{pmatrix}$, and $\begin{pmatrix} 2 \\ 1 \end{pmatrix}$. Every stress ω in G is an equilibrium stress, because the forces applied by each edge cancel out. The weighted Delaunay graph of a single point is identical for all weights, so it suffices to verify that G_1 is not an intrinsic Delaunay triangulation. We easily observe that the longest edge of G_1 is not Delaunay. See Figure 3.

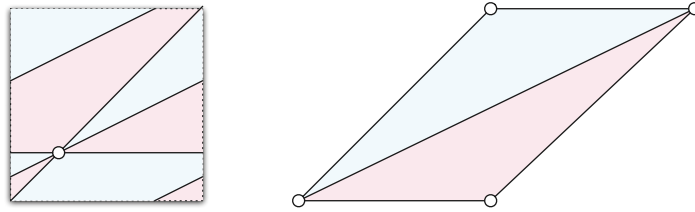


Figure 3. A one-vertex triangulation G_1 on the square flat torus, and a lift of its faces to the universal cover. Every stress in G_1 is an equilibrium stress, but G_1 is not a (weighted) intrinsic Delaunay triangulation.

More generally, for any positive integer k , let G_k denote the $k \times k$ covering of G_1 . The vertices of G_k form a regular $k \times k$ square toroidal lattice, and the edges of G_k fall into three parallel families, with displacement vectors $\begin{pmatrix} 1/k \\ 1/k \end{pmatrix}$, $\begin{pmatrix} 2/k \\ 1/k \end{pmatrix}$, and $\begin{pmatrix} 1/k \\ 0 \end{pmatrix}$. Every positive stress vector where all parallel edges have equal stress coefficients is an equilibrium stress.

For the sake of argument, suppose G_k is coherent. Let $p \rightarrow r$ be any dart with displacement vector $\begin{pmatrix} 2/k \\ 1/k \end{pmatrix}$, and let q and s be the vertices before and after r in clockwise order around p . The local Delaunay determinant test (2.2) implies that the weights of these four vertices satisfy the inequality $\pi_p + \pi_r + 1 < \pi_q + \pi_s$. Every vertex of G_k appears in exactly four inequalities of this form—twice on the left and twice on the right—so summing all k^2 such inequalities and canceling equal terms yields the obvious contradiction $1 < 0$. \square

3.1 Example

As a running example, let G be the (unweighted) intrinsic Delaunay triangulation of the seven points $(0), (\frac{1}{7}), (\frac{2}{7}), (\frac{3}{7}), (\frac{4}{7}), (\frac{5}{7}), (\frac{6}{7})$ on the square flat torus \mathbb{T}_\square , and let G^* be the corresponding intrinsic Voronoi diagram, as shown in Figure 4. The triangulation G is a highly symmetric geodesic embedding of the complete graph K_7 ; torus graphs isomorphic to G and G^* were studied in several early seminal works on combinatorial topology [38, 39, 65].

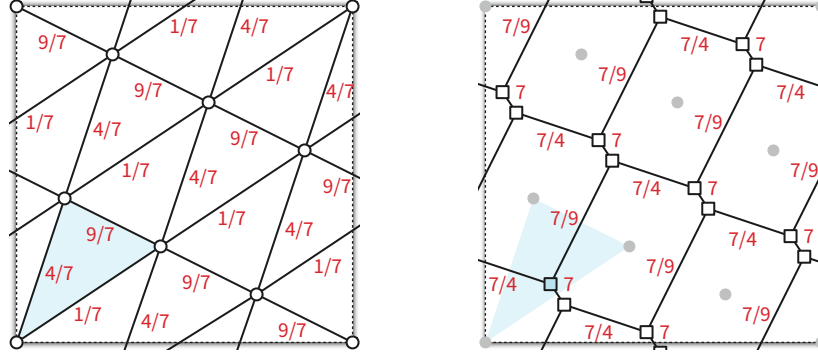


Figure 4. An intrinsic Delaunay triangulation, its dual Voronoi diagram, and their induced equilibrium stresses. Compare with Figures 5 and 6.

The edges of G fall into three equivalence classes, with slopes 3, $2/3$, $-1/2$ and lengths $\sqrt{10}/7$, $\sqrt{5}/7$, $\sqrt{14}/7$, respectively. The triangle $(0), (\frac{1}{7}), (\frac{3}{7})$, shaded in Figure 4, has circumcenter $(\frac{19}{98})$. Measuring slopes and distances to the nearby edge midpoints, we find that corresponding dual edges in G^* have slopes $-1/3$, $-3/2$, and 2 and lengths $4\sqrt{10}/49$, $\sqrt{5}/49$, and $9\sqrt{14}/49$, respectively. These dual slopes confirm that G and G^* are reciprocal (as are any Delaunay triangulation and its dual Voronoi diagram). The dual edge lengths imply that assigning stress coefficients $4/7$, $1/7$, and $9/7$ to the edges of G yields an equilibrium stress for G , and symmetrically, the stress coefficients $7/4$, 7, and $9/7$ yield an equilibrium stress for G^* .

Of course, this is not the only equilibrium stress for G ; indeed, symmetry implies that G is in equilibrium with respect to the uniform stress $\omega \equiv 1$. However, there is no reciprocal embedding G^* such that every edge in G has the same length as the corresponding dual edge in G^* .

The doubly-periodic universal cover \tilde{G} is also in equilibrium with respect to the uniform stress $\omega \equiv 1$. Thus, the classical Maxwell–Cremona correspondence implies an embedding of the dual graph $(\tilde{G})^*$ in which every dual edge is orthogonal to and has the same length as its corresponding primal edge in \tilde{G} . (Borcea and Streinu [11, Proposition 2] discuss how to solve the infinite linear system giving the heights of the corresponding polyhedral lifting of \tilde{G} .) Symmetry implies that $(\tilde{G})^*$ is doubly-periodic. Crucially, however, \tilde{G} and $(\tilde{G})^*$ have *different period lattices*. Specifically, the period lattice of $(\tilde{G})^*$ is generated by the vectors $\begin{pmatrix} 2 \\ -1 \end{pmatrix}$ and $\begin{pmatrix} -1 \\ 2 \end{pmatrix}$; see Figure 5.

Understanding which equilibrium stresses correspond to reciprocal embeddings is the topic of Section 5. In particular, in that section we describe a simple necessary and sufficient condition for an equilibrium stress to be reciprocal, which the unit stress for G fails.

4 Coherent = Reciprocal

Unlike in the previous and following sections, the equivalence between coherent graphs and graphs with reciprocal diagrams generalizes fully from the plane to the torus. However, there is an important difference from the planar setting. In both the plane and the torus, every translation of a reciprocal

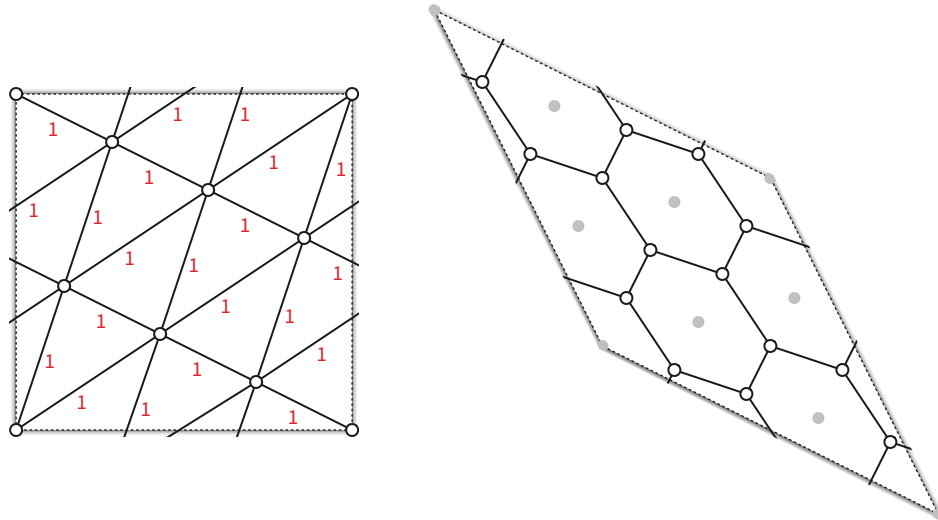


Figure 5. A “reciprocal” embedding (at half scale) induced by the uniform equilibrium stress $\omega \equiv 1$. Compare with Figures 4 and 6.

diagram is another reciprocal diagram. For a coherent plane graph G , every reciprocal diagram is a weighted Voronoi diagram of the vertices of G , but *exactly one* reciprocal diagram of a coherent torus graph G is a weighted Voronoi diagram of the vertices of G . Said differently, every coherent plane graph is a weighted Delaunay graph with respect to a three-dimensional space of vertex weights, which correspond to translations of any convex polyhedral lifting, but every coherent *torus* graph is a weighted Delaunay graph with respect to only a *one*-dimensional space of vertex weights.

4.1 Notation

In this section we fix a non-singular matrix $M = (u, v)$ where $u, v \in \mathbb{R}^2$ are column vectors and $\det M > 0$, and consider a torus graph G on \mathbb{T}_M . We primarily work with the universal cover \tilde{G} of G ; if we are given a reciprocal embedding G^* , we also work with its universal cover \tilde{G}^* (which is reciprocal to \tilde{G}). Vertices in \tilde{G} are denoted by the letters p and q and treated as column vectors in \mathbb{R}^2 . A generic face in \tilde{G} is denoted by the letter f ; the corresponding dual vertex in \tilde{G}^* is denoted f^* and interpreted as a row vector. To avoid nested subscripts when darts are indexed, we write $\Delta_i = \Delta_{d_i}$ and $\omega_i = \omega_{d_i}$, and therefore by Lemma 3.1, $\Delta_i^* = \omega_i \Delta_i^\perp$. For any integers a and b , the translation $p + au + bv$ of any vertex p of \tilde{G} is another vertex of \tilde{G} , and the translation $f + au + bv$ of any face f of \tilde{G} is another face of \tilde{G} . It follows that $(f + au + bv)^* = f^* + au^T + bv^T$.

4.2 Results

The following lemma follows directly from the definitions of weighted Delaunay graphs and their dual weighted Voronoi diagrams; see, for example, Aurenhammer [4, 6].

Lemma 4.1. *Let G be a weighted Delaunay graph on some flat torus \mathbb{T}_M , and let G^* be the corresponding weighted Voronoi diagram on \mathbb{T} . Every edge e of G is orthogonal to its dual e^* . In short, every coherent torus graph is reciprocal.*

The converse of this lemma is false; unlike in the plane, a reciprocal diagram G^* for a torus graph G is *not* necessarily a weighted Voronoi diagram of the vertices of G . Rather, as we describe below, a unique translation of G^* is such a weighted Voronoi diagram.

Maxwell's theorem implies a convex polyhedral lifting $z: \mathbb{R}^2 \rightarrow \mathbb{R}$ of the universal cover \tilde{G} of G , where the gradient vector $\nabla z|_f$ within any face f is equal to the coordinate vector of the dual vertex f^* in \tilde{G}^* . To make this lifting unique, we fix a vertex o of \tilde{G} to lie at the origin $\begin{pmatrix} 0 \\ 0 \end{pmatrix}$, and we require $z(o) = 0$.

Define the weight of each vertex $p \in \tilde{G}$ as

$$\pi_p = \frac{1}{2}|p|^2 - z(p).$$

By definition, $\pi_o = 0$. The determinant conditions (2.2) and (2.3) for an edge e to be locally Delaunay are both equivalent to interpreting $\frac{1}{2}|p|^2 - \pi_p$ as a z -coordinate and requiring that the induced lifting be locally convex at e . Because z is a convex polyhedral lifting, these weights establish that \tilde{G} is the intrinsic weighted Delaunay graph of its vertex set.

Translating the universal cover \tilde{G}^* of the reciprocal graph G^* adds a global linear term to the lifting function z , and therefore to the Delaunay weights π_p . The main result of this section is that there is a unique translation such that the corresponding Delaunay weights π_p are periodic.

To compute $z(q)$ for any point $q \in \mathbb{R}^2$, we choose an arbitrary face f of \tilde{G} that contains q and identify the equation $z|_f(q) = \eta q + c$ of the plane through the lift of f , where $\eta \in \mathbb{R}^2$ is a row vector and $c \in \mathbb{R}$. Borcea and Streinu [11] give a calculation for η and c , which for our setting can be written as follows:

Lemma 4.2 (Borcea and Streinu [11, Eq. 7]). *For $q \in \mathbb{R}^2$, let f be a face containing q . The function $z|_f$ can be explicitly computed as follows:*

- Pick an arbitrary **root** face f_0 incident to o .
- Pick an arbitrary path from f_0^* to f^* in \tilde{G}^* , and let d_1^*, \dots, d_ℓ^* be the dual darts along this path. By definition, we have $f^* = f_0^* + \sum_{i=1}^\ell \Delta_i^*$. Set $C(f) = \sum_{i=1}^\ell \omega_i |p_i q_i|$, where $d_i = p_i \rightarrow q_i$ and $|p_i q_i| = \det(p_i, q_i)$.
- Set $\eta = f^*$ and $c = C(f)$, implying that $z|_f(q) = f^* q + C(f)$. In particular, $C(f)$ is the intersection of this plane with the z -axis.

Reciprocity of \tilde{G}^* implies that the actual choice of root face f_0^* and the path to f^* do not matter. We use this explicit computation to establish the existence of a translation of G^* such that $\pi_o = \pi_u = \pi_v = 0$. We then show that after this translation, every lift of the same vertex of G has the same Delaunay weight.

Lemma 4.3. *There is a unique translation of \tilde{G}^* such that $\pi_o = \pi_u = \pi_v = 0$. Specifically, this translation places the dual vertex of the root face f_0 at the point*

$$f_0^* = \left(-\frac{1}{2}(|u|^2, |v|^2) - (C(f_0 + u), C(f_0 + v)) \right) M^{-1}.$$

Proof: Lemma 4.2 implies that

$$z(u) = (f_0 + u)^* u + C(f_0 + u) = f_0^* u + |u|^2 + C(f_0 + u),$$

and by definition, $\pi_u = 0$ if and only if $z(u) = \frac{1}{2}|u|^2$. Thus, $\pi_u = 0$ if and only if $f_0^* u = -\frac{1}{2}|u|^2 - C(f_0 + u)$. A symmetric argument implies $\pi_v = 0$ if and only if $f_0^* v = -\frac{1}{2}|v|^2 - C(f_0 + v)$. \square

Lemma 4.4. *If $\pi_o = \pi_u = \pi_v = 0$, then $\pi_p = \pi_{p+u} = \pi_{p+v}$ for all $p \in V(\tilde{G})$. In other words, all lifts of any vertex of G have equal weight.*

Proof: Let f be any face incident to p , and let $P = d_1^*, \dots, d_\ell^*$ be an arbitrary path from f_0^* to f^* in \tilde{G}^* . We compute $C(f+u)$ by traversing an arbitrary path from f_0^* to $(f_0+u)^* = f_0^* + u^T$ followed by the translated path $P+u$ from $f_0^* + u^T$ to $f^* + u^T$. Thus by Lemma 4.2, $C(f+u) = C(f_0+u) + \sum_{i=1}^\ell \omega_i |(p_i + u) \cdot (q_i + u)|$, and $f^* = f_0^* + \sum_{i=1}^\ell \Delta_i^*$. We thus have

$$\begin{aligned} C(f+u) &= C(f_0+u) + \sum_{i=1}^\ell \omega_i |(p_i + u) \cdot (q_i + u)| \\ &= C(f_0+u) + \sum_{i=1}^\ell \omega_i |p_i \cdot q_i| - \sum_{i=1}^\ell \Delta_i^* u \\ &= C(f_0+u) + C(f) - \sum_{i=1}^\ell \Delta_i^* u \\ &= -\frac{1}{2}|u|^2 - f_0^* u + C(f) - \sum_{i=1}^\ell \Delta_i^* u \\ &= -\frac{1}{2}|u|^2 - f^* u + C(f). \end{aligned}$$

It follows that

$$\begin{aligned} \pi_{p+u} &= \frac{1}{2}|p+u|^2 - z(p+u) \\ &= \frac{1}{2}|p+u|^2 - (C(f+u) + (f^* + u^T)(p+u)) \\ &= \frac{1}{2}|p+u|^2 - \left(-\frac{1}{2}|u|^2 - f^* u + C(f) + f^* p + f^* u + u^T p + |u|^2\right) \\ &= \frac{1}{2}|p+u|^2 - z(p) - \frac{1}{2}|u|^2 - u^T p \\ &= \frac{1}{2}|p|^2 + \frac{1}{2}|u|^2 + u^T p - z(p) - \frac{1}{2}|u|^2 - u^T p \\ &= \frac{1}{2}|p|^2 - z(p) \\ &= \pi_p. \end{aligned}$$

A similar computation implies $\pi_{p+v} = \pi_p$. □

Projecting from the universal cover back to the torus, we obtain weights for the vertices of G , with respect to which G is an intrinsic weighted Delaunay complex, and a unique translation of G^* that is the corresponding intrinsic weighted Voronoi diagram. Moreover, these Delaunay vertex weights are unique if we fix the weight of an arbitrary vertex of G to be 0.

Theorem 4.5. *Let G and G^* be reciprocal geodesic graphs on some flat torus \mathbb{T}_M . G is a weighted Delaunay complex, and a unique translation of G^* is the corresponding weighted Voronoi diagram. In short, every reciprocal torus graph is coherent.*

5 Equilibrium Implies Reciprocal, Sort Of

Now fix an essentially simple, essentially 3-connected geodesic graph G on the *square* flat torus \mathbb{T}_\square , along with a positive equilibrium stress ω for G . In this section, we describe simple necessary and sufficient conditions for ω to be a reciprocal stress for G . More generally, we show that there is an essentially unique flat torus \mathbb{T}_M such that a unique scalar multiple of ω is a reciprocal stress for the image of G on \mathbb{T}_M .

Let Δ be the $2 \times E$ displacement matrix of G , and let Ω be the $E \times E$ matrix whose diagonal entries are $\Omega_{e,e} = \omega_e$ and whose off-diagonal entries are all 0. The results in this section are phrased in terms of the covariance matrix $\Delta\Omega\Delta^T = \begin{pmatrix} \alpha & \gamma \\ \gamma & \beta \end{pmatrix}$, where

$$\alpha = \sum_e \omega_e \Delta x_e^2, \quad \beta = \sum_e \omega_e \Delta y_e^2, \quad \gamma = \sum_e \omega_e \Delta x_e \Delta y_e. \quad (5.1)$$

Recall that $A^\perp = (JA)^T$.

5.1 The Square Flat Torus

Before considering arbitrary flat tori, as a warmup we first establish necessary and sufficient conditions for ω to be a reciprocal stress for G on the *square* flat torus \mathbb{T}_\square , in terms of the parameters α , β , and γ .

Lemma 5.1. *If ω is a reciprocal stress for G on \mathbb{T}_\square , then $\Delta\Omega\Delta^T = \begin{pmatrix} 1 & 0 \\ 0 & 1 \end{pmatrix}$.*

Proof: Suppose ω is a reciprocal stress for G on \mathbb{T}_\square . Then there is a geodesic embedding of the dual graph G^* on \mathbb{T}_\square where $e \perp e^*$ and $|e^*| = \omega_e |e|$ for every edge e of G . Let $\Delta^* = (\Delta\Omega)^\perp$ denote the $E \times 2$ matrix whose rows are the displacement row vectors of G^* .

Recall from Lemma 2.5 that the first and second rows of Λ describe cocirculations of G with cohomology classes $(0, 1)$ and $(-1, 0)$, respectively. Applying Lemma 2.1 to G^* implies $\theta\Delta^* = [\theta]^*$ for any cocirculation θ in G . It follows immediately that $\Lambda\Delta^* = \begin{pmatrix} 0 & 1 \\ -1 & 0 \end{pmatrix} = -J$.

Because the rows of Δ^* are the displacement vectors of G^* , for every vertex p of G we have

$$\sum_{q: pq \in E} \Delta_{(p \rightarrow q)^*}^* = \sum_{d: \text{tail}(d)=p} \Delta_{d^*}^* = \sum_{d: \text{left}(d^*)=p^*} \Delta_{d^*}^* = (0, 0). \quad (5.2)$$

It follows that the *columns* of Δ^* describe circulations in G . Lemma 2.1 now implies that $\Delta\Delta^* = -J$. We conclude that $\Delta\Omega\Delta^T = \Delta\Delta^*J = \begin{pmatrix} 1 & 0 \\ 0 & 1 \end{pmatrix}$. \square

Lemma 5.2. *Fix an $E \times 2$ matrix Δ^* . If $\Lambda\Delta^* = -J$, then Δ^* is the displacement matrix of a geodesic drawing on \mathbb{T}_\square that is dual to G . Moreover, if that drawing has an equilibrium stress, it is actually an embedding.*

Proof: Let λ_1 and λ_2 denote the rows of Λ . Rewriting the identity $\Lambda\Delta^* = -J$ in terms of these row vectors gives us $\sum_e \Delta_e^* \lambda_{1,e} = (0, 1) = [\lambda_1]^*$ and $\sum_e \Delta_e^* \lambda_{2,e} = (-1, 0) = [\lambda_2]^*$. Extending by linearity, we have $\sum_e \Delta_e^* \theta_e = [\theta]^*$ for every cocirculation θ in G^* . The result now follows from Lemma 2.4. \square

Lemma 5.3. *If $\Delta\Omega\Delta^T = \begin{pmatrix} 1 & 0 \\ 0 & 1 \end{pmatrix}$, then ω is a reciprocal stress for G on \mathbb{T}_\square .*

Proof: Set $\Delta^* = (\Delta\Omega)^\perp$. Because ω is an equilibrium stress in G , for every vertex p of G we have

$$\sum_{q: pq \in E} \Delta_{(p \rightarrow q)^*}^* = \sum_{q: pq \in E} \omega_{pq} \Delta_{p \rightarrow q}^\perp = (0, 0). \quad (5.3)$$

It follows that the columns of Δ^* describe circulations in G , and therefore Lemma 2.1 implies $\Lambda\Delta^* = \Delta\Delta^* = \Delta(\Delta\Omega)^\perp = \Delta\Omega\Delta^T J^T = -J$.

Lemma 5.2 now implies that Δ^* is the displacement matrix of a drawing G^* dual to G . Moreover, the stress vector ω^* defined by $\omega_{e^*}^* = 1/\omega_e$ is an equilibrium stress for G^* : under this stress vector, the darts leaving any dual vertex f^* are dual to the clockwise boundary cycle of face f in G . Thus G^* is in fact an embedding. By construction, each edge of G^* is orthogonal to the corresponding edge of G . \square

5.2 Force Diagrams

The results of the previous section have a more physical interpretation that may be more intuitive. Let G be any geodesic graph on the unit square flat torus \mathbb{T}_{\square} . Recall from Section 3.1 that any positive stress ω on G induces a positive stress on its universal cover \tilde{G} , which in turn induces a reciprocal diagram $(\tilde{G})^*$ by the classical Maxwell–Cremona correspondence. This infinite plane graph $(\tilde{G})^*$ is doubly-periodic, but in general with a different period lattice from the universal cover \tilde{G} .

Said differently, we can always construct another geodesic torus graph H that is combinatorially dual to G , such that for every edge e of G , the corresponding edge e^* of H is orthogonal to e and has length $\omega_e \cdot |e|$; however, this torus graph H does not necessarily lie on the *square* flat torus. (By construction, H is the unique torus graph whose universal cover is $(\tilde{G})^*$, the reciprocal diagram of the universal cover of G .) We call H the **force diagram** of G with respect to ω . The force diagram H lies on the same flat torus \mathbb{T}_{\square} as G if and only if ω is a reciprocal stress for G .

Lemma 5.4. *Let G be a geodesic graph in \mathbb{T}_{\square} , and let ω be a positive equilibrium stress for G . The force diagram of G with respect to ω lies on the flat torus \mathbb{T}_M , where $M = \begin{pmatrix} \beta & -\gamma \\ -\gamma & \alpha \end{pmatrix} = J\Delta\Omega\Delta^T J^T$.*

Proof: As usual, let Δ be the displacement matrix of G . Let Δ^* denote the displacement matrix of the force diagram H ; by definition, we have $\Delta^* = (\Delta\Omega)^{\perp} = \Omega\Delta^T J^T$. Equation (5.3) implies that the columns of Δ^* are circulations in G . Thus, Lemma 2.1 implies that $\Lambda\Delta^* = \Delta\Delta^* = \Delta\Omega\Delta^T J^T$.

Set $M = J\Delta\Delta^* = J\Delta\Omega\Delta^T J^T = \begin{pmatrix} \beta & -\gamma \\ -\gamma & \alpha \end{pmatrix}$. We immediately have $\Lambda\Delta^* = J^{-1}M = -JM = -JM^T$ and therefore $\Lambda\Delta^*(M^T)^{-1} = -J$. Lemma 5.2 implies that $\Delta^*(M^T)^{-1}$ is the displacement matrix of a homotopic embedding of G^* on \mathbb{T}_{\square} . It follows that Δ^* is the displacement matrix of the image of G^* on \mathbb{T}_M . We conclude that H is a translation of the image of G^* on \mathbb{T}_M . \square

5.3 Arbitrary Flat Tori

Now we generalize our previous analysis to graphs on the flat torus \mathbb{T}_M defined by an arbitrary non-singular matrix $M = \begin{pmatrix} a & b \\ c & d \end{pmatrix}$. These results are also stated in terms of the parameters α , β , and γ , which are still defined in terms of \mathbb{T}_{\square} , which will serve as a *reference* flat torus when talking about flat tori defined by different non-singular matrices.

Lemma 5.5. *If ω is a reciprocal stress for a geodesic graph G on \mathbb{T}_M , then $\alpha\beta - \gamma^2 = 1$; in particular, if $M = \begin{pmatrix} a & b \\ c & d \end{pmatrix}$, then*

$$\alpha = \frac{b^2 + d^2}{ad - bc}, \quad \beta = \frac{a^2 + c^2}{ad - bc}, \quad \gamma = \frac{-(ab + cd)}{ad - bc}.$$

For example, if $M = (u, v)$ where $u, v \in \mathbb{R}^2$ are column vectors and $\det M = 1$, then $\Delta\Omega\Delta^T = \begin{pmatrix} v \cdot v & -u \cdot v \\ -u \cdot v & u \cdot u \end{pmatrix}$.

Proof: Suppose ω is a reciprocal stress for G on \mathbb{T}_M . Then there is a geodesic embedding of the dual graph G^* on \mathbb{T}_M where $e \perp e^*$ and $|e^*| = \omega_e |e|$ for every edge e of G .

It will prove convenient to consider the geometry of G and G^* on the reference torus \mathbb{T}_{\square} . (The embeddings of G and G^* on the reference torus \mathbb{T}_{\square} are still dual, but not necessarily reciprocal.) Let Δ denote the $2 \times E$ reference displacement matrix for G , whose columns are the displacement vectors for G on the square torus \mathbb{T}_{\square} . Then the columns of $M\Delta$ are the *native* displacement vectors for G on the torus \mathbb{T}_M . Thus, the *native* displacement row vectors of G^* are given by the rows of the $E \times 2$ matrix $(M\Delta\Omega)^{\perp}$. Finally, let $\Delta^* = (M\Delta\Omega)^{\perp}(M^T)^{-1}$ denote the *reference* displacement row vectors for G^* on

the square torus \mathbb{T}_\square . We can rewrite this definition as

$$\begin{aligned}
 \Delta^* &= (M\Delta\Omega)^\perp (M^T)^{-1} \\
 &= (M\Delta\Omega)^\perp (M^{-1})^T \\
 &= (JM\Delta\Omega)^T (M^{-1})^T \\
 &= \Omega\Delta^T M^T J^T (M^{-1})^T,
 \end{aligned} \tag{5.4}$$

which implies $\Omega\Delta^T = \Delta^* M^T J (M^{-1})^T$.

Because the rows of Δ^* are the displacement vectors for G^* , equation (5.2) implies that the *columns* of Δ^* describe circulations in G , and therefore $\Delta\Delta^* = \Lambda\Delta^* = \begin{pmatrix} 0 & 1 \\ -1 & 0 \end{pmatrix} = -J$ by Lemmas 2.1 and 2.5. We conclude that

$$\begin{aligned}
 \Delta\Omega\Delta^T &= \Delta\Delta^* M^T J (M^{-1})^T = J^T M^T J (M^{-1})^T \\
 &= \frac{1}{ad-bc} \begin{pmatrix} 0 & 1 \\ -1 & 0 \end{pmatrix} \begin{pmatrix} a & c \\ b & d \end{pmatrix} \begin{pmatrix} 0 & -1 \\ 1 & 0 \end{pmatrix} \begin{pmatrix} d & -c \\ -b & a \end{pmatrix} \\
 &= \frac{1}{ad-bc} \begin{pmatrix} b & d \\ -a & -c \end{pmatrix} \begin{pmatrix} b & -a \\ d & -c \end{pmatrix} \\
 &= \frac{1}{ad-bc} \begin{pmatrix} b^2 + d^2 & -ab - cd \\ -ab - cd & a^2 + c^2 \end{pmatrix}.
 \end{aligned}$$

Routine calculation now implies that $\alpha\beta - \gamma^2 = \det \Delta\Omega\Delta^T = 1$. □

Corollary 5.6. *If ω is a reciprocal stress for G on \mathbb{T}_M , then $M = \sigma R \begin{pmatrix} \beta & -\gamma \\ 0 & 1 \end{pmatrix}$ for some 2×2 rotation matrix R and some real number $\sigma > 0$.*

Proof: Reciprocity is preserved by rotating and scaling the fundamental parallelogram \diamond_M , so it suffices to consider the special case $M = \begin{pmatrix} a & b \\ 0 & 1 \end{pmatrix}$. In this special case, Lemma 5.5 immediately implies $\beta = a$ and $\gamma = -b$. □

Lemma 5.7. *If $\alpha\beta - \gamma^2 = 1$, then ω is a reciprocal stress for G on \mathbb{T}_M where $M = \sigma R \begin{pmatrix} \beta & -\gamma \\ 0 & 1 \end{pmatrix}$ for any 2×2 rotation matrix R and any real number $\sigma > 0$.*

Proof: Suppose $\alpha\beta - \gamma^2 = 1$. Fix an arbitrary 2×2 rotation matrix R and an arbitrary real number $\sigma > 0$, and let $M = \sigma R \begin{pmatrix} \beta & -\gamma \\ 0 & 1 \end{pmatrix}$. Let Δ denote the $2 \times E$ reference displacement matrix for G on the square flat torus \mathbb{T}_\square , and define the $E \times 2$ matrix $\Delta^* = (M\Delta\Omega)^\perp (M^T)^{-1}$.

Derivation (5.4) in the proof of Lemma 5.5 implies $\Delta^* = \Omega\Delta^T (M^{-1}JM)^T$. We easily observe that $(\sigma R)^{-1}J(\sigma R) = J$, and therefore

$$\begin{aligned}
 M^{-1}JM &= \begin{pmatrix} \beta & -\gamma \\ 0 & 1 \end{pmatrix}^{-1} \begin{pmatrix} 0 & -1 \\ 1 & 0 \end{pmatrix} \begin{pmatrix} \beta & -\gamma \\ 0 & 1 \end{pmatrix} \\
 &= \frac{1}{\beta} \begin{pmatrix} 1 & \gamma \\ 0 & \beta \end{pmatrix} \begin{pmatrix} 0 & -1 \\ 1 & 0 \end{pmatrix} \begin{pmatrix} \beta & -\gamma \\ 0 & 1 \end{pmatrix} \\
 &= \frac{1}{\beta} \begin{pmatrix} \beta\gamma & -1 - \gamma^2 \\ \beta^2 & -\beta\gamma \end{pmatrix} \\
 &= \begin{pmatrix} \gamma & -\alpha \\ \beta & -\gamma \end{pmatrix}.
 \end{aligned}$$

It follows that

$$\Delta\Delta^* = \Delta\Omega\Delta^T(M^{-1}JM)^T = \begin{pmatrix} \alpha & \gamma \\ \gamma & \beta \end{pmatrix} \begin{pmatrix} \gamma & \beta \\ -\alpha & -\gamma \end{pmatrix} = \begin{pmatrix} 0 & \alpha\beta - \gamma^2 \\ \gamma^2 - \alpha\beta & 0 \end{pmatrix} = -J.$$

Because ω is an equilibrium stress in G , for every vertex p of G we have

$$\sum_{q: pq \in E} \Delta_{(p \rightarrow q)^*}^* = \sum_{q: pq \in E} \omega_{pq} \Delta_{p \rightarrow q}^\perp (M^{-1}JMJ^T)^T = (0,0)(M^{-1}JMJ^T)^T = (0,0). \quad (5.5)$$

Once again, the columns of Δ^* describe circulations in G , so Lemma 2.1 implies $\Lambda\Delta^* = \Delta\Delta^* = -J$. Lemma 5.2 now implies that Δ^* is the displacement matrix of a homotopic embedding of G^* on \mathbb{T}_\square . It follows that $(M\Delta\Omega)^\perp = \Delta^*M^T$ is the displacement matrix of the image of G^* on \mathbb{T}_M . By construction, each edge of G^* is orthogonal to its corresponding edge of G . We conclude that ω is a reciprocal stress for G . \square

Our main theorem now follows immediately.

Theorem 5.8. *Let G be a geodesic graph on \mathbb{T}_\square with positive equilibrium stress ω . Let α , β , and γ be defined as in Equation (5.1). If $\alpha\beta - \gamma^2 = 1$, then ω is a reciprocal stress for the image of G on \mathbb{T}_M if and only if $M = \sigma R \begin{pmatrix} \beta & -\gamma \\ 0 & 1 \end{pmatrix}$ for any rotation matrix R and any real number $\sigma > 0$. On the other hand, if $\alpha\beta - \gamma^2 \neq 1$, then ω is not a reciprocal stress for the image of G on any flat torus.*

In short, every equilibrium graph on any flat torus has a coherent affine image on *some* essentially unique flat torus. The requirement $\alpha\beta - \gamma^2 = 1$ is a necessary scaling condition: Given any equilibrium stress ω , the scaled equilibrium stress $\omega/\sqrt{\alpha\beta - \gamma^2}$ satisfies the requirement.²

The results of this section can be reinterpreted in terms of force diagrams as follows:

Lemma 5.9. *Let G be a geodesic graph on \mathbb{T}_M , and let ω be a positive equilibrium stress for G . The force diagram of G with respect to ω lies on the flat torus \mathbb{T}_N , where $N = JM\Delta\Omega\Delta^TJ^T$.*

Proof: We argue exactly as in the proof of Lemma 5.4. Let Δ be the *reference* displacement matrix of (the image of) G on \mathbb{T}_\square . Then the *native* displacement matrix of the force diagram is $\Delta^* = (M\Delta\Omega)^\perp = \Omega\Delta^T M^T J^T$. Equation (5.5) and Lemma 2.1 imply that $\Lambda\Delta^* = \Delta\Omega\Delta^T M^T J^T$.

Now let $N = JM\Delta\Omega\Delta^TJ^T$. We immediately have $J^{-1}N^T = \Lambda\Delta^*$ and thus $\Lambda\Delta^*(N^T)^{-1} = J^{-1} = -J$. Lemma 5.2 implies that $\Delta^*(N^T)^{-1}$ is the displacement matrix of a homotopic embedding of G^* on \mathbb{T}_\square . It follows that Δ^* is the displacement matrix of the image of G^* on \mathbb{T}_N . \square

5.4 Example

Let us revisit once more the example graph G from Section 3.1: the symmetric embedding of K_7 on the square flat torus \mathbb{T}_\square . Symmetry implies that G is in equilibrium with respect to the uniform stress $\omega \equiv 1$. Straightforward calculation gives us the parameters $\alpha = \beta = 2$ and $\gamma = 1$ for this stress vector. Thus, Lemma 5.1 immediately implies that ω is not a reciprocal stress for G ; rather, by Lemma 5.4, the force diagram of G with respect to ω lies on the torus \mathbb{T}_M , where $M = \begin{pmatrix} \beta & -\gamma \\ -\gamma & \alpha \end{pmatrix} = \begin{pmatrix} 2 & -1 \\ -1 & 2 \end{pmatrix}$. Moreover, because $\alpha\beta - \gamma^2 = 3 \neq 1$, Lemma 5.5 implies that ω is not a reciprocal stress for the image of G on *any* flat torus. In short, there are no reciprocal embeddings of G and G^* on *any* flat torus such that corresponding primal and dual edges have equal length.

²Note that $\alpha\beta - \gamma^2 = \frac{1}{2} \sum_{e,e'} \omega_e \omega_{e'} \left| \frac{\Delta x_e}{\Delta x_{e'}} \frac{\Delta y_e}{\Delta y_{e'}} \right|^2 > 0$.

Now consider the scaled uniform stress $\omega \equiv 1/\sqrt{3}$, which has parameters $\alpha = \beta = 2/\sqrt{3}$ and $\gamma = 1/\sqrt{3}$. This new stress ω is still not a reciprocal stress for G ; however, it does satisfy the scaling constraint $\alpha\beta - \gamma^2 = 1$. Lemma 5.5 (or Lemma 5.9) implies that ω is a reciprocal stress for the image of G on the flat torus \mathbb{T}_M , where $M = \frac{1}{\sqrt{3}} \begin{pmatrix} 2 & -1 \\ 0 & \sqrt{3} \end{pmatrix}$. The fundamental parallelogram \diamond_M is the union of two equilateral triangles with height 1. Not surprisingly, the image of G on \mathbb{T}_M is a Delaunay triangulation with equilateral triangle faces, and the faces of the reciprocal Voronoi diagram G^* (which is also the force diagram) are regular hexagons. Finally, the vector $\omega^* \equiv \sqrt{3}$ is a reciprocal stress, and therefore an equilibrium stress, for G^* . See Figure 6.

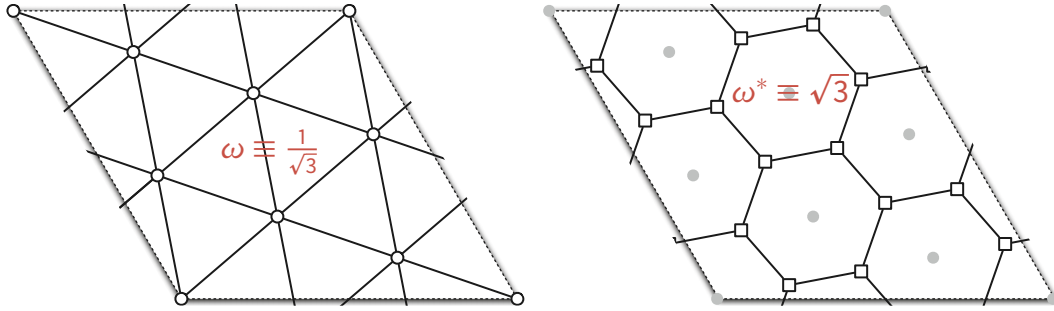


Figure 6. A seven-vertex Delaunay triangulation and its dual Voronoi diagram, induced by the uniform stress $1/\sqrt{3}$; compare with Figures 4 and 5.

6 A Toroidal Steinitz Theorem

Finally, Theorem 2.3 and Theorem 5.8 immediately imply a natural generalization of Steinitz’s theorem to graphs on the flat torus.

Theorem 6.1. *Let G be any essentially simple, essentially 3-connected embedded graph on the square flat torus \mathbb{T}_{\square} , and let ω be **any** positive stress on the edges of G . Then G is homotopic to a geodesic embedding in \mathbb{T}_{\square} whose image in some flat torus \mathbb{T}_M is coherent.*

As we mentioned in the introduction, Mohar’s generalization [61] of the Koebe-Andreev circle packing theorem already implies that every essentially simple, essentially 3-connected torus graph G is homotopic to *one* coherent homotopic embedding on *one* flat torus. In contrast, our results characterize *all* coherent homotopic embeddings of G on *all* flat tori. Every positive stress vector $\omega \in \mathbb{R}^E$ corresponds to an essentially unique coherent homotopic embedding of G , which is unique up to translation, on a flat torus \mathbb{T}_M , which is unique up to similarity of the fundamental parallelogram \diamond_M . On the other hand, Lemmas 3.1 and 4.1 imply that every coherent embedding of G on every flat torus corresponds to a unique positive equilibrium stress.

Acknowledgements. We thank the anonymous reviewers of the SOCG version of this paper [33] for their helpful comments and suggestions.

References

- [1] E. M. Andreev. [Convex polyhedra in Lobachevskii space](#). *Mat. Sbornik* 10(3):413–440, 1970.
- [2] E. M. Andreev. [On convex polyhedra of finite volume in Lobachevskii space](#). *Mat. Sbornik* 12(2):270–259, 1970.

- [3] Franz Aurenhammer. [A criterion for the affine equivalence of cell complexes in \$R^d\$ and convex polyhedra in \$R^{d+1}\$](#) . *Discrete Comput. Geom.* 2(1):49–64, 1987.
- [4] Franz Aurenhammer. [Power diagrams: Properties, algorithms and applications](#). *SIAM J. Comput.* 16(1):78–96, 1987.
- [5] Franz Aurenhammer. [Recognising polytopical cell complexes and constructing projection polyhedra](#). *J. Symb. Comput.* 3(3):249–255, 1987.
- [6] Franz Aurenhammer and Hiroshi Imai. [Geometric relations among Voronoi diagrams](#). *Geom. Dedicata* 27(1):65–75, 1988.
- [7] Alexander I. Bobenko and Boris A. Springborn. [A discrete Laplace-Beltrami operator for simplicial surfaces](#). *Discrete Comput. Geom.* 38(4):740–756, 2007.
- [8] Mikhail Bogdanov, Monique Teillaud, and Gert Vegter. [Delaunay triangulations on orientable surfaces of low genus](#). *Proc. 32nd Int. Symp. Comput. Geom.*, 20:1–20:17, 2016. Leibniz Int. Proc. Informatics 51.
- [9] Ciprian Borcea and Ileana Streinu. [Periodic frameworks and flexibility](#). *Proc. Royal Soc. A* 466(2121):2633–2649, 2010.
- [10] Ciprian Borcea and Ileana Streinu. [Minimally rigid periodic graphs](#). *Bull. London Math. Soc.* 43(6):1093–1103, 2011.
- [11] Ciprian Borcea and Ileana Streinu. [Liftings and stresses for planar periodic frameworks](#). *Discrete Comput. Geom.* 53(4):747–782, 2015.
- [12] Graham R. Brightwell and Edward R. Scheinerman. [Representations of planar graphs](#). *SIAM J. Discrete Math.* 6(2):214–229, 1993.
- [13] Kevin Q. Brown. [Voronoi diagrams from convex hulls](#). *Inform. Process. Lett.* 9(5):223–228, 1979.
- [14] Manuel Caroli and Monique Teillaud. [Delaunay triangulations of closed Euclidean \$d\$ -orbifolds](#). *Discrete Comput. Geom.* 55(4):827–853, 2016.
- [15] Marek Chrobak, Michael T. Goodrich, and Roberto Tamassia. [Convex drawings of graphs in two and three dimensions \(preliminary version\)](#). *Proc. 12th Ann. Symp. Comput. Geom.*, 319–328, 1996.
- [16] Yves Colin de Verdière. [Empilements de cercles: Convergence d’une méthode de point fixe](#). *Forum Math.* 1(1):395–402, 1989.
- [17] Yves Colin de Verdière. [Sur un nouvel invariant des graphes et un critère de planarité](#). *J. Comb. Theory Ser. B* 50(1):11–21, 1990. In French, English translation in [20].
- [18] Yves Colin de Verdière. [Comment rendre géodésique une triangulation d’une surface?](#) *L’Enseignement Mathématique* 37:201–212, 1991.
- [19] Yves Colin de Verdière. [Un principe variationnel pour les empilements de cercles](#). *Invent. Math.* 104(1):655–669, 1991.
- [20] Yves Colin de Verdière. [On a new graph invariant and a criterion for planarity](#). *Graph Structure Theory*, 137–147, 1993. Contemporary Mathematics 147, Amer. Math. Soc. English translation of [17] by Neil Calkin.

- [21] Éric Colin de Verdière and Arnaud de Mesmay. [Testing graph isotopy on surfaces](#). *Discrete Comput. Geom.* 51(1):171–206, 2014.
- [22] Robert Connelly, Erik D. Demaine, and Günter Rote. Infinitesimally locked self-touching linkages with applications to locked trees. *Physical Knots: Knotting, Linking, and Folding of Geometric Objects in \mathbb{R}^3* , 287–311, 2002. Amer. Math. Soc.
- [23] Keenan Crane. *Discrete Differential Geometry: An Applied Introduction*. 2019. (<http://www.cs.cmu.edu/~kmc Crane/Projects/DDG/paper.pdf>).
- [24] Henry Crapo and Walter Whiteley. Plane self stresses and projected polyhedra I: The basic pattern. *Topologie structurale / Structural Topology* 20:55–77, 1993. (<http://hdl.handle.net/2099/1091>).
- [25] Luigi Cremona. *Le figure reciproche nella statica grafica*. Tipografia di Giuseppe Bernardoni, 1872. (http://www.luigi-cremona.it/download/Scritti_matematici/1872_statica_grafica.pdf). English translation in [26].
- [26] Luigi Cremona. *Graphical Statics*. Oxford Univ. Press, 1890. (<https://archive.org/details/graphicalstatico2cremgoog>). English translation of [25] by Thomas Hudson Beare.
- [27] Jesús De Loera, Jörg Rambau, and Francisco Santos. *Triangulations: Structures for Algorithms and Applications*. Algorithms and Computation in Mathematics 25. Springer, 2010.
- [28] Olaf Delgado-Friedrichs. [Equilibrium placement of periodic graphs and convexity of plane tilings](#). *Discrete Comput. Geom.* 33(1):67–81, 2004.
- [29] Erik D. Demaine and Joseph O’Rourke. *Geometric Folding Algorithms: Linkages, Origami, Polyhedra*. Cambridge Univ. Press, 2007.
- [30] Erik D. Demaine and André Schulz. [Embedding stacked polytopes on a polynomial-size grid](#). *Discrete Comput. Geom.* 57(4):782–809, 2017.
- [31] Peter Eades and Patrick Garvan. [Drawing stressed planar graphs in three dimensions](#). *Proc. 2nd Symp. Graph Drawing*, 212–223, 1995. Lecture Notes Comput. Sci. 1027.
- [32] Herbert Edelsbrunner and Raimund Seidel. [Voronoi diagrams and arrangements](#). *Discrete Comput. Geom.* 1(1):25–44, 1986.
- [33] Jeff Erickson and Patrick Lin. [A toroidal Maxwell-Cremona-Delaunay correspondence](#). *Proc. 36rd Int. Symp. Comput. Geom.*, 40:1–40:17, 2020. Leibniz Int. Proc. Informatics, Schloss Dagstuhl–Leibniz-Zentrum für Informatik.
- [34] Stefan Felsner and Günter Rote. [On Primal-Dual Circle Representations](#). *Proc. 2nd Symp. Simplicity in Algorithms*, 8:1–8:18, 2018. OpenAccess Series in Informatics (OASICS) 69, Schloss Dagstuhl–Leibniz-Zentrum für Informatik.
- [35] Daniel Gonçalves and Benjamin Lévêque. [Toroidal maps: Schnyder woods, orthogonal surfaces and straight-line representations](#). *Discrete Comput. Geom.* 51(1):67–131, 2014.
- [36] Steven J. Gortler, Craig Gotsman, and Dylan Thurston. [Discrete one-forms on meshes and applications to 3D mesh parameterization](#). *Comput. Aided Geom. Design* 23(2):83–112, 2006.
- [37] Clara I. Grima and Alberto Márquez. *Computational Geometry on Surfaces*. Springer, 2001.

- [38] Percy John Heawood. Map colour theorems. *Quart. J. Pure Appl. Math.* 24:332–338, 1890. (<https://babel.hathitrust.org/cgi/pt?id=inu.30000050138159&seq=344>).
- [39] Lothar Heffter. Ueber das Problem der Nachbargebiete. *Math. Ann.* 38(4):477–508, 1891.
- [40] John E. Hopcroft and Peter J. Kahn. A paradigm for robust geometric algorithms. *Algorithmica* 7(1–6):339–380, 1992.
- [41] David Huffman. A duality concept for the analysis of polyhedral scenes. *Machine Intelligence*, vol. 8, 475–492, 1977. Ellis Horwood Ltd. and John Wiley & Sons.
- [42] Alexander Igambardiev and André Schulz. A duality transform for constructing small grid embeddings of 3d polytopes. *Comput. Geom. Theory Appl.* 56:19–36, 2016.
- [43] Hiroshi Imai, Masao Iri, and Kazuo Murota. Voronoi diagram in the Laguerre geometry and its applications. *SIAM J. Comput.* 14(1):93–105, 1985.
- [44] Clause Indermitte, Thomas M. Liebling, Marc Troyanov, and Heinz Clemençon. Voronoi diagrams on piecewise flat surfaces and an application to biological growth. *Theoret. Comput. Sci.* 263(1–2):263–274, 2001.
- [45] Ivan Izvestiev. Statics and kinematics of frameworks in Euclidean and non-Euclidean geometry. *Eighteen Essays in Non-Euclidean Geometry*, 2019. IRMA Lectures in Mathematics and Theoretical Physics 29, Europ. Math. Soc.
- [46] Paul Koebe. Kontaktprobleme der Konformen Abbildung. *Ber. Sächs. Akad. Wiss. Leipzig, Math.-Phys. Kl.* 88:141–164, 1936.
- [47] Andrew Kotlov, László Lovász, and Santosh Vempala. The Colin de Verdière number and sphere representations of a graph. *Combinatorica* 17(4):483–521, 1997.
- [48] Yves Ladegaillie. Classification topologique des plongements des 1-complexes compacts dans les surfaces. *C. R. Acad. Sci. Paris A* 278:1401–1403, 1974. (<https://gallica.bnf.fr/ark:/12148/bpt6k6236784g/f179>).
- [49] Yves Ladegaillie. Classification topologique des plongements des 1-complexes compacts dans les surfaces. *C. R. Acad. Sci. Paris A* 279:129–132, 1974. (<https://gallica.bnf.fr/ark:/12148/bpt6k6238171d/f143>).
- [50] Yves Ladegaillie. Classes d’isotopie de plongements de 1-complexes dans les surfaces. *Topology* 23(3):303–311, 1984.
- [51] Charles L. Lawson. Transforming triangulations. *Discrete Math.* 3(4):365–372, 1972.
- [52] László Lovász. Representations of polyhedra and the Colin de Verdière number. *J. Comb. Theory Ser. B* 82(2):223–236, 2001.
- [53] László Lovász. Discrete analytic functions: An exposition. *Eigenvalues of Laplacians and other geometric operators*, 241–273, 2004. Surveys in Differential Geometry 9, Int. Press.
- [54] László Lovász. *Graphs and Geometry*. Colloquium Publications 69. Amer. Math. Soc., 2019.
- [55] James Clerk Maxwell. On reciprocal figures and diagrams of forces. *Phil. Mag. (Ser. 4)* 27(182):250–261, 1864.

- [56] James Clerk Maxwell. On the application of the theory of reciprocal polar figures to the construction of diagrams of forces. *Engineer* 24:402, 1867. Reprinted in [58, pp. 313–316].
- [57] James Clerk Maxwell. On reciprocal figures, frames, and diagrams of forces. *Trans. Royal Soc. Edinburgh* 26(1):1–40, 1870.
- [58] James Clerk Maxwell. *The Scientific Letters and Papers of James Clerk Maxwell. Volume 2: 1862–1873*. Cambridge Univ. Press, 2009.
- [59] Maria Mazón and Tomás Recio. Voronoi diagrams on orbifolds. *Comput. Geom. Theory Appl.* 8(5):219–230, 1997.
- [60] Bojan Mohar. A polynomial time circle packing algorithm. *Discrete Math.* 117(1–3):257–263, 1993.
- [61] Bojan Mohar. Circle packings of maps—The Euclidean case. *Rend. Sem. Mat. Fis. Milano* 67(1):191–206, 1997.
- [62] Bojan Mohar. Circle packings of maps in polynomial time. *Europ. J. Combin.* 18(7):785–805, 1997.
- [63] Bojan Mohar and Pierre Rosenstiehl. Tessellation and visibility representations of maps on the torus. *Discrete Comput. Geom.* 19(2):249–263, 1998.
- [64] Bojan Mohar and Alexander Schrijver. Blocking nonorientability of a surface. *J. Comb. Theory Ser. B* 87(1):2–16, 2003.
- [65] August F. Möbius. Zur Theorie der Polyëder und der Elementarverwandtschaft [Nachlass]. *Gesammelte Werke*, vol. 2, 515–559, 1886. Hirzel, Leipzig. (<http://gallica.bnf.fr/ark:/12148/bpt6k994243/f524>).
- [66] Shmuel Onn and Bernd Sturmfels. A quantitative Steinitz’ theorem. *Beitr. Algebra Geom.* 35(1):125–129, 1994. (<https://www.emis.de/journals/BAG/vol.35/no.1/>).
- [67] David Orden, Günter Rote, Fransisco Santos, Brigitte Servatius, Herman Servatius, and Walter Whiteley. Non-crossing frameworks with non-crossing reciprocals. *Discrete Comput. Geom.* 32(4):567–600, 2004.
- [68] W. J. Macquorn Rankine. Principle of the equilibrium of polyhedral frams. *London, Edinburgh, and Dublin Phil. Mag J. Sci.* 27(180):92, 1864.
- [69] William John Macquorn Rankine. *A Manual of Applied Mechanics*. Richard Griffin and Co., 1858. (<https://archive.org/details/manualappmechaoorankrich>).
- [70] Ares Ribó Mor, Günter Rote, and André Schulz. Small grid embeddings of 3-polytopes. *Discrete Comput. Geom.* 45(1):65–87, 2011.
- [71] Jürgen Richter-Gebert. *Realization spaces of polytopes*. Lecture Notes Math. 1643. Springer, 1996.
- [72] Igor Rivin. Euclidean structures on simplicial surfaces and hyperbolic volume. *Ann. Math.* 139:553–580, 1994.
- [73] Günter Rote, Fransisco Santos, and Ileana Streinu. Pseudo-triangulations—a survey. *Essays on Discrete and Computational Geometry: Twenty Years Later*, 343–410, 2008. Contemporary Mathematics 453, Amer. Math. Soc.

- [74] André Schulz. [Drawing 3-polytopes with good vertex resolution](#). *J. Graph Algorithms Appl.* 15(1):33–52, 2011.
- [75] Dvir Steiner and Anath Fischer. Planar parameterization for closed 2-manifold genus-1 meshes. *Proc. 9th ACM Symp. Solid Modeling Appl.*, 83–91, 2004.
- [76] Ernst Steinitz. Polyeder und Raumeinteilungen. *Enzyklopädie der mathematischen Wissenschaften mit Einschluss ihrer Anwendungen* III.AB(12):1–139, 1916.
- [77] Ernst Steinitz and Hans Rademacher. *Vorlesungen über die Theorie der Polyeder: unter Einschluß der Elemente der Topologie*. Grundlehren der mathematischen Wissenschaften 41. Springer-Verlag, 1934. Reprinted 1976.
- [78] Kenneth Stephenson. *Introduction to Circle Packing: The Theory of Discrete Analytic Functions*. Cambridge Univ. Press, 2005.
- [79] Ileana Streinu. [Erratum to “Pseudo-triangulations, rigidity and motion planning”](#). *Discrete Comput. Geom.* 35(2):358, 2006.
- [80] Ileana Streinu. [Pseudo-triangulations, rigidity and motion planning](#). *Discrete Comput. Geom.* 34(4):587–635, 2006. Publisher’s erratum in [79].
- [81] Kokichi Sugihara. Realizability of polyhedrons from line drawings. *Computational Morphology: A Computational Geometric Approach to the Analysis Of Form*, 177–206, 1988. Machine Intelligence and Pattern Recognition 6.
- [82] William T. Tutte. [How to draw a graph](#). *Proc. London Math. Soc.* 13(3):743–768, 1963.
- [83] Pierre Varignon. *Nouvelle mécanique ou statique, dont le projet fut donné en M.DC.LXXVII*. Claude Jombert, Paris, 1725. (<https://gallica.bnf.fr/ark:/12148/bpt6k5652714w.texteImage>).
- [84] Georges F. Voronoï. Nouvelles applications des paramètres continus à la théorie des formes quadratiques. Deuxième mémoire. Recherches sur les paralléloèdres primitifs. *J. Reine Angew. Math.* 134:198–287, 1908. (<https://eudml.org/doc/149291>).
- [85] Walter Whiteley. Motion and stresses of projected polyhedra. *Topologie structurale / Structural Topology* 7:13–38, 1982. (<http://hdl.handle.net/2099/989>).
- [86] Walter Whiteley, Peter F. Ash, Ethan Poiker, and Henry Crapo. [Convex polyhedra, Dirichlet tessellations, and spider webs](#). *Shaping Space: Exploring Polyhedra in Nature, Art, and the Geometrical Imagination*, chapter 18, 231–251, 2013. Springer.
- [87] Günter M. Ziegler. *Lectures on Polytopes*. Graduate Texts in Mathematics 152. Springer, 1995.